Nanochem Res 6(2): 248-255, Summer and Autumn 2021

RESEARCH PAPER

Biosynthesis and catalytic activity of Pd/$NiFe_2O_4$ nanocomposite for the reduction of wastewater pollutants

Akbar Rostami-Vartooni[1*], Mojtaba Bagherzadeh[2*], Mohaddeseh Sajjadi[1], Ahmad Reza Abbasian[3]

[1] Department of Chemistry, Faculty of Science, University of Qom, Iran

[2] Reactor and Nuclear Safety School, Nuclear Science and Technology Research Institute, Isfahan, Iran

[3] Department of Materials Engineering, Faculty of Engineering, University of Sistan and Baluchestan, Zahedan, Iran

ARTICLE INFO

Article History:
Received 01 July 2021
Accepted 18 September 2021
Published 15 October 2021

Keywords:
Pd nanoparticles
$NiFe_2O_4$ nanoparticles
M. vulgare L
Catalytic Reduction

ABSTRACT

In the present work, the preparation of nickel ferrite ($NiFe_2O_4$) and its surface modification by biosynthesized Pd nanoparticles (NPs) were carried out. Firstly, $NiFe_2O_4$ NPs were synthesized via a facile combustion approach and then Pd NPs were biosynthesized on their surface by using an aqueous *Marrubium vulgare L* leaf extract. The prepared $NiFe_2O_4$ NPs were characterized by FT-IR, XRD, VSM, FESEM, and EDXA techniques, which confirmed the good dispersion of spherical Pd NPs on the surface of magnetic NiFe2O4 nanoparticles. The catalytic activity of Pd/NiFe2O4 nanocomposites were evaluated in the reduction of Methylene Blue (MB), Methyl Orange (MO) and Congo Red (CR) azo dyes in the presence of sodium borohydride ($NaBH_4$). Observed results showed that the reduction/decolorization times in the presence of magnetically recoverable Pd/$NiFe_2O_4$ nanocomposites were very shorter than that of $NiFe_2O_4$ catalyst.

How to cite this article
Rostami-Vartooni A., Bagherzadeh M., Sajjadi M., Abbasian A.R.. Biosynthesis and catalytic activity of Pd/$NiFe_2O_4$ nanocomposite for the reduction of wastewater pollutants. Nanochem Res, 2021; 6(2):248-255. DOI: 10.22036/ncr.2021.02.011

INTRODUCTION

Dyes as water and wastewater pollutants are produced from textiles, plastics, paper, leather, food, and cosmetics industries. Different methods such as adsorption, advanced oxidation processes (AOPs), chemical reduction, biological degradation, ion exchange, membrane separation and coagulation [1-3] have been employed to remove these carcinogenic and mutagenic compounds. In the current decade, the reduction/decolorization process including $NaBH_4$ as a reducing agent has been reported to convert the pollutants to less toxic materials [4-6].

The usage of metal nanoparticles (MNPs) has been significantly studied in recent years due to their high specific surface area and good catalytic activity [7, 8]. Specifically, Pd NPs have been widely used in various chemical reactions such as coupling reactions, selective oxidation of alcohols, arylation of phenols and reduction of water/wastewater pollutants [9, 10]. Immobilization of MNPs on the surface of different supports such as reduced graphene oxide, Fe_3O_4, bentonite, TiO_2, CuO, perlite, and seashell decreases the agglomeration of NPs which leads to stable catalysts with higher reactivity and good reusability [11, 12]. However, metal ferrites with inverse spinel structure, such as $NiFe_2O_4$, have been synthesized via different methods including co-precipitation [13], sol-gel [14], chemical reduction [15], hydrothermal [16], microwave combustion, and sonochemical methods [17].

Among several physical, chemical and biological approaches for the preparation of MNPs, biosynthetic route using plant extracts has some advantages including the elimination of toxic and

* Corresponding Author Email: *a.rostami@qom.ac.ir*
mjmo123@yahoo.com

expensive chemical compounds and providing gentle reaction conditions [18-25]. The phenolic compounds are present in different parts of plants, which can act as reducing and stabilizing agents for the conversion of metal ions to MNPs.

Marrubium vulgare L as a traditional plant has been used in the treatments of liver diseases, cancer and diabetes mellitus due to its antioxidant properties [26]. In addition, this medicinal plant has several pharmaceutical activities such as antibacterial, anti-inflammatory, antihypertensive, vasodilator, hypolipidemic, wound-healing and sedative potential [27, 28]. The flowers and fruits of *M. vulgare L* are good sources of tannins, amino acids and polysaccharides, whereas phenols and flavonoids are the major constituents of leaves [29, 30].

In the present study, biosynthesized Pd NPs by using the aqueous leaf extract of *M. vulgare L.* were supported on the surface of magnetically recoverable $NiFe_2O_4$ prepared by combustion method. This biofabricated Pd/$NiFe_2O_4$ nanocomposite was applied for the catalytic reduction of MB, MO and CR dyes.

EXPERIMENTAL METHOD

Materials and instruments

The leaves of *Marrubium vulgare L.* were collected from Isfahan province (Josheghan-Ghali city), Iran. Nickle ferrite ($NiFe_2O_4$) was prepared based on previously reported procedure by using $Ni(NO_3)_2.6H_2O$, $Fe(NO_3)_3.9H_2O$, glycine, and KCl salt [31]. Other required materials were purchased from Merck®. The reduction reactions of water/wastewater pollutants were studied by a Lambda-35 UV-Vis spectrophotometer (PerkinElmer, United States). FT-IR spectra of the $NiFe_2O_4$ and its Pd nanocomposite were recorded by Cary 630 FTIR spectrometer. The XRD measurements were performed using a Philips PW 1730 X-ray diffractometer with CuKa radiation (λ=0.154 nm) to identify the phase composition of nanocomposites. The morphology and structure of Pd/$NiFe_2O_4$ nanocomposite was characterized by FESEM analysis (Cam scan MV2300) equipped with an energy-dispersive X-ray analysis (EDX). The magnetic property of the $NiFe_2O_4$ was investigated by a SQUID magnetometer (Quantum Design MPMS XL).

Preparation of $NiFe_2O_4$ nanocomposite

$NiFe_2O_4$ was synthesized via combustion method reported by Abbasian and Afarani [32]. Firstly, the pH of 60 ml distilled water was adjusted to 4 by adding HNO_3 and then 4.44 mmol glycine solution was added to this media in a beaker (250 ml). After that, 10 mmol of $Ni(NO_3)_2$ was dissolved in the solution prepared in the previus section and agitated. Equal mmol of $Fe(NO_3)_3$ and KCl (20 mmol) were added to them under magnetic stirring for 15 min intervals at 80 °C. The resulting solution was agitated under magnetic stirring at 200 °C on the magnetic stirrer until the color of the solution changed to brown. Finally, heating was continued without stirring until the combustion reaction occurred and the dark brownish powder was produced. The obtained powders were boiled in about 400 ml of distilled water to remove unreacted KCl. The gained powders were separated by using a piece of magnet and dried at 80 °C in an electric oven. The prepared materials ($NiFe_2O_4$) were used as a catalyst.

Preparation of M. vulgare L leaf extract

The *M. vulgare L.* reagent were extracted from 6 g of leaves in 80 mL of deionized water and heated at 75 °C for 20 min. Finally, the filtered extract was used in the formation of Pd NPs.

Synthesis of Pd/$NiFe_2O_4$ nanocomposite

A solution containing 0.2 g $PdCl_2$ dissolved in 0.5 M HCl was added to a mixture of 1.2 g $NiFe_2O_4$ and 30 mL *M. vulgare L.* leaf extract. After 1.5 h, the obtained Pd/$NiFe_2O_4$ nanocomposite was separated using a magnet, washed with deionized water and placed in an oven at 100 °C for 30 min.

Catalytic reduction of MB, MO and CR using Pd/$NiFe_2O_4$ nanocomposite

4 mg of $NiFe_2O_4$ or its Pd nanocomposite was added to an aqueous solution of MB or MO dye (90 mL, 10 ppm) and $NaBH_4$ (5 mg). The mixture was then stirred at room temperature and the reduction/decolorization process was monitored by UV-Vis absorption spectrometer at λ_{max} of 664, 464 and 493 nm for measuring MB, MO and CR concentrations, respectively.

RESULTS AND DISCUSSION

Pd NPs synthesis

Scheme 1 shows that the phenolic compounds in the *M. vulgare L* leaf extract are responsible for the Pd NPs formation and stabilization [3, 33]. Immobilization of these nanoparticles on the

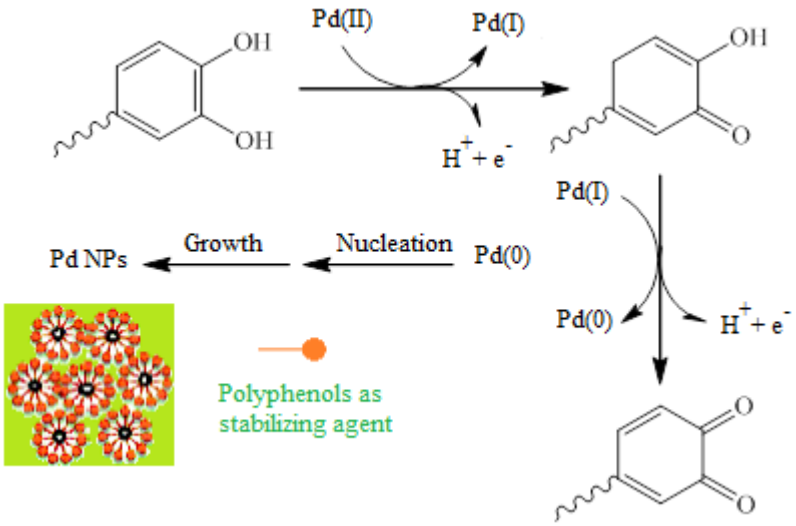

Scheme 1. The Pd NPs preparation by using the *M. vulgare L* leaf extract.

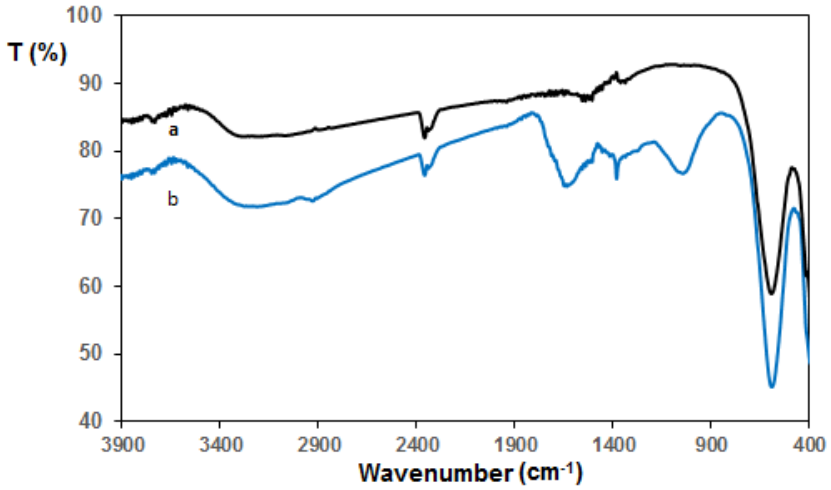

Fig. 1. FT-IR spectra of $NiFe_2O_4$ (a) and Pd/$NiFe_2O_4$ (b).

$NiFe_2O_4$ leads to more stable Pd NPs and high catalyst activity.

Characterization of the Ni ferrite and its Pd nanocomposite

The formation of $NiFe_2O_4$ support can be confirmed by the observed peaks at about 400 and 594 cm^{-1} in its FT-IR spectrum (Fig. 1) which are attributed to the stretching vibrations of metal–oxygen bands in the octahedral and tetrahedral sites, respectively [34, 35]. The broad band in the range of 3000-3400 cm^{-1} is assigned to the existence of surface O–H bond and absorbed H_2O by the ferrite sample. The absorption bands at 930-1645 cm^{-1} in the FTIR spectrum of Pd/$NiFe_2O_4$ nanocomposite (Fig. 1b) can be related to the C–O and C=C bonds of absorbed phenolic constituents in the aqueous extract on the nanocomposite surface by π-electron interactions [36, 37].

XRD pattern of Ni ferrite (Fig. 2) is completely compatible with the reported pattern in the literature [38-40]. The diffraction peaks at 2θ values of 30.5, 35.9, 37.4, 43.7, 53.8, 57.4, 63.0, 71.5, 74.6, 75.7 and 79.5° (Card No. 89–4927) can be easily indexed to the (220), (311), (222), (400), (422), (511), (440), (620), (533), (622) and (444) planes of cubic spinel $NiFe_2O_4$ (JCPDS PDF card no.10-0325), respectively. The observed peaks at 2θ values

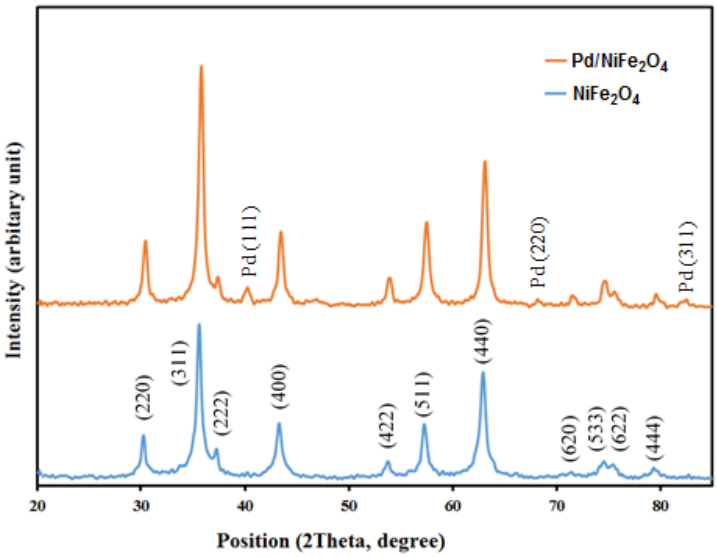

Fig. 2. XRD patterns of $NiFe_2O_4$ (a) and Pd/$NiFe_2O_4$ nanocomposite (b).

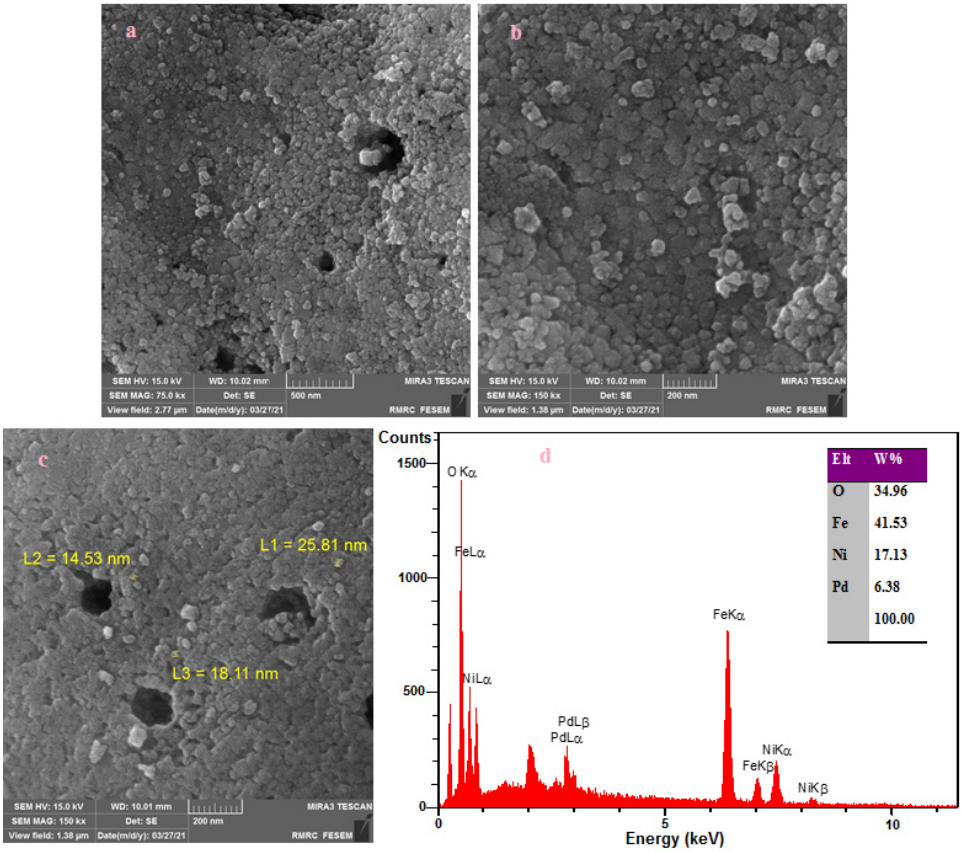

Fig. 3. The (a-c) FESEM images and (d) EDX spectrum of Pd/$NiFe_2O_4$ nanocomposite.

of 40.1, 68.3 and 82.5° in the XRD pattern of Pd/$NiFe_2O_4$ are related to the (111), (220) and (311) planes of crystalline Pd with the face-centered cubic structure [41, 42].

The FESEM images of Pd/$NiFe_2O_4$ nanocomposite (Fig. 3a-c) show that the produced spherical Pd NPs have dispersed well on the surface of magnetic support. EDX spectrum of Pd/$NiFe_2O_4$

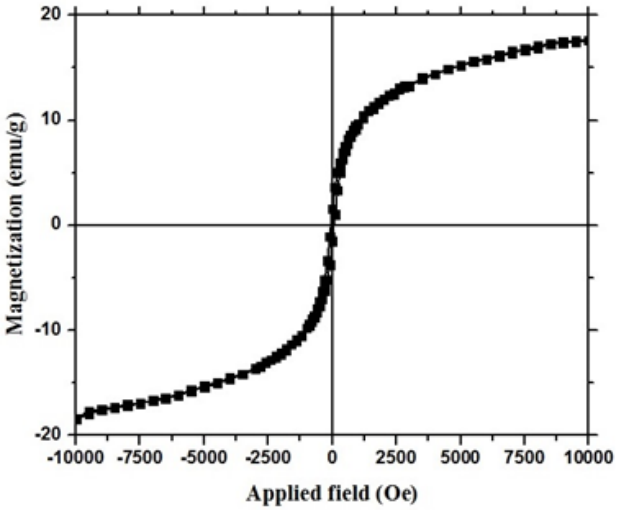

Fig. 4. Magnetization curve of the $NiFe_2O_4$ nanocomposite.

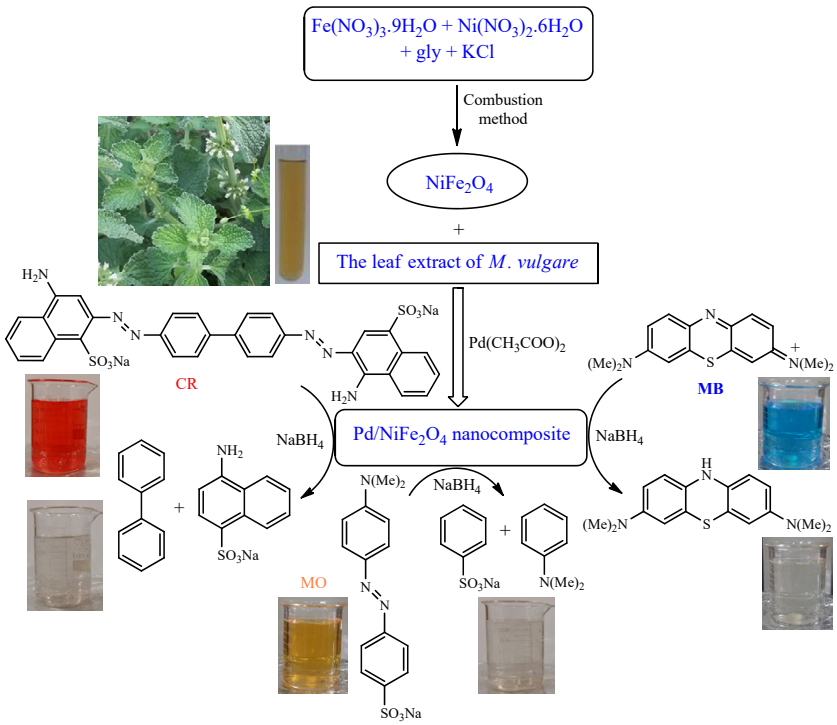

Scheme 2. Green synthesis of Pd/$NiFe_2O_4$ nanocomposite and its catalytic evaluation in the reduction of MO, MB and CR.

(Fig. 3d) confirms the presence of Pd, Ni, Fe and O elements in this nanocomposite.

Fig. 4 shows the value of saturation magnetization (Ms) for the prepared $NiFe_2O_4$ nanocomposite with ferromagnetic behavior is about 17.5 emu/g. This magnitude of magnetization was sufficient for the facile separation of the nanocomposite from the reactions by an external magnet.

Application of the Ni ferrite and its Pd NPs nanocomposite in the reduction of dyes

Reduction/decolorization process of azo dyes as *pollutants* in the presence of $NaBH_4$ was chosen for the investigation of catalytic activity of the Pd/$NiFe_2O_4$ nanocomposite (Scheme 2). In these reduction reactions, the color of MB, MO and CR solutions completely disappeared. The reduction

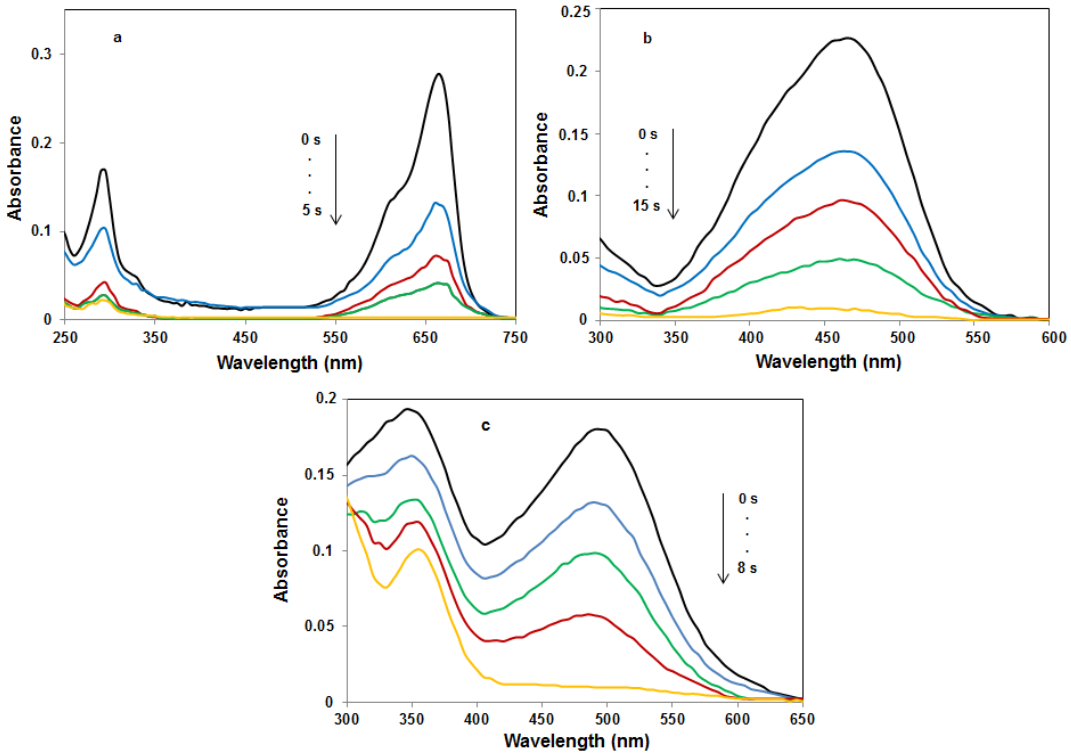

Fig. 5. Absorption intensities of MB (a), MO (b) and CR (c) solutions during the catalytic reduction.

Table 1. Reduction times of selected dyes (90 mL, 10.0 ppm) in the presence of catalyst (4 mg) using $NaBH_4$ (5 mg).

Catalyst	MB	MO	CR
-	90 min[a]	90 min[a]	90 min[a]
$NiFe_2O_4$	90 min[b]	90 min[b]	90 min[b]
$Pd/NiFe_2O_4$	120 min[c]	120 min[c]	120 min[c]
$Pd/NiFe_2O_4$	5 s	15 s	8 s

[a]No reaction; [b]Not completed; [c]Without $NaBH_4$.

products of MO and CR remained unchanged even when the reactions were continued up to 24 h. Nevertheless, the re-oxidation of the reduced form of MB occurred and the color of the solution returned to the original blue color after 3 h. Fig. 5 shows the changes of absorption intensities in UV-vis spectra of MB, MO and CR solutions at different time intervals. In addition, the reduction times of the pollutants in different conditions are summarized in Table 1. In the presence of $Pd/NiFe_2O_4$ catalyst, shorter reaction times were observed which indicated the electron transfer from the reducing agent (BH_4^-) to pollutants as a rate-limiting step (rds) were facilitated on the surface of Pd NPs [43]. It could be found from the reaction times listed in Table 1, the efficiency of $Pd/NiFe_2O_4$ nanocomposite are comparable to the reported catalysts in the literature for the reduction/decolorization of pollutants [6, 43-46].

Catalyst recyclability

To investigate the recyclability of the catalyst, the separated $Pd/NiFe_2O_4$ from MO reaction using external magnet was washed with distilled water, dried and then reused in the reduction process. The reaction times of 100% MO reduction/decolorization for 4 catalytic runs were 15, 16, 20 and 20 s, respectively. Hence, the efficiency of the recovered catalyst does not change significantly, indicating the appropriate stability of the $Pd/NiFe_2O_4$ catalyst.

CONCLUSIONS

In the first step of this work, Ni ferrite

nanocomposite prepared by hydrothermal process was selected as a stable and magnetically recoverable support for the biofabricated Pd NPs using *M. vulgare L leaves* extract. The formation $NiFe_2O_4$ and its Pd nanocomposite was confirmed by FTIR, VSM, XRD, FESEM and EDS techniques. The FESEM images and EDS spectrum showed the immobilization of well-dispersed spherical Pd NPs on the surface of the magnetic $NiFe_2O_4$ support. The reduction/decolorization process of MB, MO and CR dyes was fully carried out in the presence of Pd/$NiFe_2O_4$.

ACKNOWLEDGEMENTS

The authors thank the NSTRI and University of Qom for financial supports of this work.

CONFLICTS OF INTEREST

The authors declare that there are no conflicts of interest regarding the publication of this paper.

REFERENCES

[1] Talat-Mehrabad J, Partovi M, Arjomandi Rad F, Khalilnezhad R. Nitrogen doped TiO_2 for efficient visible light photocatalytic dye degradation. Iranian Journal of Catalysis. 2019;9(3):233-9.

[2] Nezamzadeh-Ejhieh A, Karimi-Shamsabadi M. Comparison of photocatalytic efficiency of supported CuO onto micro and nano particles of zeolite X in photodecolorization of Methylene blue and Methyl orange aqueous mixture. Applied Catalysis A: General. 2014;477:83-92.

[3] Nasrollahzadeh M, Sajadi SM, Maham M. Green synthesis of palladium nanoparticles using Hippophae rhamnoides Linn leaf extract and their catalytic activity for the Suzuki–Miyaura coupling in water. Journal of Molecular Catalysis A: Chemical. 2015;396:297-303.

[4] Rostami-Vartooni A, Moradi-Saadatmand A, Mahdavi M. Catalytic reduction of organic pollutants using biosynthesized Ag/C/Fe_3O_4 nanocomposite by red water and Caesalpinia gilliesii flower extract. Materials Chemistry and Physics. 2018;219:328-39.

[5] Wang G, Zhao K, Gao C, Wang J, Mei Y, Zheng X, et al. Green synthesis of copper nanoparticles using green coffee bean and their applications for efficient reduction of organic dyes. Journal of Environmental Chemical Engineering. 2021;9(4):105331.

[6] Bordbar M, Negahdar N, Nasrollahzadeh M. Melissa Officinalis L. leaf extract assisted green synthesis of CuO/ZnO nanocomposite for the reduction of 4-nitrophenol and Rhodamine B. Separation and Purification Technology. 2018;191:295-300.

[7] Subhan F, Aslam S, Yan Z, Yaseen M, Marwat A, Ahmad A. Catalytic reduction of nitrophenol and MB waste water using homogeneous Pt NPs confined in hierarchically porous silica. Journal of Environmental Chemical Engineering. 2021;9(4):105567.

[8] Alkhalayfeh MA, Aziz AA, Pakhuruddin MZ. Enhancing the efficiency of polymer solar cells by embedding Au@Ag NPs Durian shape in buffer layer. Solar Energy. 2021;214:565-74.

[9] Khodadadi B, Bordbar M, Nasrollahzadeh M. Green synthesis of Pd nanoparticles at Apricot kernel shell substrate using Salvia hydrangea extract: Catalytic activity for reduction of organic dyes. Journal of Colloid and Interface Science. 2017;490:1-10.

[10] Nasrollahzadeh M, Sajadi SM, Rostami-Vartooni A, Bagherzadeh M. Green synthesis of Pd/CuO nanoparticles by Theobroma cacao L. seeds extract and their catalytic performance for the reduction of 4-nitrophenol and phosphine-free Heck coupling reaction under aerobic conditions. Journal of Colloid and Interface Science. 2015;448:106-13.

[11] Nasrollahzadeh M, Maham M, Rostami-Vartooni A, Bagherzadeh M, Sajadi SM. Barberry fruit extract assisted in situ green synthesis of Cu nanoparticles supported on a reduced graphene oxide–Fe_3O_4 nanocomposite as a magnetically separable and reusable catalyst for the O-arylation of phenols with aryl halides under ligand-free conditions. RSC Advances. 2015;5(79):64769-80.

[12] Rostami-Vartooni A, Rostami L, Bagherzadeh M. Green synthesis of Fe3O4/bentonite-supported Ag and Pd nanoparticles and investigation of their catalytic activities for the reduction of azo dyes. Journal of Materials Science: Materials in Electronics. 2019;30(24):21377-87.

[13] Maaz K, Karim S, Mumtaz A, Hasanain SK, Liu J, Duan JL. Synthesis and magnetic characterization of nickel ferrite nanoparticles prepared by co-precipitation route. Journal of Magnetism and Magnetic Materials. 2009;321(12):1838-42.

[14] Sen R, Jain P, Patidar R, Srivastava S, Rana RS, Gupta N. Synthesis and Characterization of Nickel Ferrite ($NiFe_2O_4$) Nanoparticles Prepared by Sol- Gel Method. Materials Today: Proceedings. 2015;2(4):3750-7.

[15] Carta D, Loche D, Mountjoy G, Navarra G, Corrias A. NiFe2O4 Nanoparticles Dispersed in an Aerogel Silica Matrix: An X-ray Absorption Study. The Journal of Physical Chemistry C. 2008;112(40):15623-30.

[16] Praveena K, Murthty SR. Magneto acoustical emission in nanocrystalline Mn–Zn ferrites. Materials Research Bulletin. 2013;48(11):4826-33.

[17] Karakas İH. The effects of fuel type onto the structural, morphological, magnetic and photocatalytic properties of nanoparticles in the synthesis of cobalt ferrite nanoparticles with microwave assisted combustion method. Ceramics International. 2021;47(4):5597-609.

[18] Rostami-Vartooni A, Nasrollahzadeh M, Salavati-Niasari M, Atarod M. Photocatalytic degradation of azo dyes by titanium dioxide supported silver nanoparticles prepared by a green method using Carpobrotus acinaciformis extract. Journal of Alloys and Compounds. 2016;689:15-20.

[19] Nasrollahzadeh M, Issaabadi Z, Sajadi SM. Green synthesis of the Ag/Al2O3 nanoparticles using Bryonia alba leaf extract and their catalytic application for the degradation of organic pollutants. Journal of Materials Science: Materials in Electronics. 2019;30(4):3847-59.

[20] Murthy HCAA. Green Silver Nanoparticles Synthesised Using Medicinal plant Echinops sp. Root Extract for Antimicrobial Applications. Nanochemistry Research. 2020;5(2):128-40.

[21] Tahmasebi zade Damirchi ¦, Rostami Charati F, Akbari R, Daneshvar A. Green synthesis of silver nanoparticles using the aqueous extract of Viscum album Fruit. Nanochemistry

Research. 2020;5(1):104-10.
[22] Ghotekar S. Plant extract mediated biosynthesis of Al_2O_3 nanoparticles- a review on plant parts involved, characterization and applications. Nanochemistry Research. 2019;4(2):163-9.
[23] Taghavi Fardood S, Moradnia F, Mostafaei M, Afshari Z, Faramarzi V, Ganjkhanlu S. Biosynthesis of $MgFe_2O_4$ magnetic nanoparticles and its application in photo-degradation of malachite green dye and kinetic study. Nanochemistry Research. 2019;4(1):86-93.
[24] Sorbiun M, Shayegan Mehr E, Ramazani A, Mashhadi Malekzadeh A. Biosynthesis of metallic nanoparticles using plant extracts and evaluation of their antibacterial properties. Nanochemistry Research. 2018;3(1):1-16.
[25] Rajabi HR, Deris H, Faraji HS. A Facile and Green Biosynthesis of Silver Nanostructures by Aqueous Extract of Suaeda Acuminata after Microwave Assisted Extraction. Nanochemistry Research. 2016;1(2):177-82.
[26] Sayyari Z, Farahmandfar R. Stabilization of sunflower oil with pussy willow (Salix aegyptiaca) extract and essential oil. Food Science & Nutrition. 2017;5(2):266-72.
[27] Rezgui M, Majdoub N, Mabrouk B, Baldisserotto A, Bino A, Ben Kaab LB, et al. Antioxidant and antifungal activities of marrubiin, extracts and essential oil from Marrubium vulgare L. against pathogenic dermatophyte strains. Journal de Mycologie Médicale. 2020;30(1):100927.
[28] El Bardai S, Lyoussi B, Wibo M, Morel N. Comparative Study of the Antihypertensive Activity of Marrubium Vulgare and of the Dihydropyridine Calcium Antagonist Amlodipine in Spontaneously Hypertensive Rat. Clinical and Experimental Hypertension. 2004;26(6):465-74.
[29] Boulila A, Sanaa A, Salem IB, Rokbeni N, M'Rabet Y, Hosni K, et al. Antioxidant properties and phenolic variation in wild populations of Marrubium vulgare L. (Lamiaceae). Industrial Crops and Products. 2015;76:616-22.
[30] Amessis-Ouchemoukh N, Abu-Reidah IM, Quirantes-Piné R, Madani K, Segura-Carretero A. Phytochemical profiling, in vitro evaluation of total phenolic contents and antioxidant properties of Marrubium vulgare (horehound) leaves of plants growing in Algeria. Industrial Crops and Products. 2014;61:120-9.
[31] Abbasian AR, Rahmani M. Salt-assisted solution combustion synthesis of nanostructured $ZnFe_2O_4$-ZnS powders. Inorganic Chemistry Communications. 2020;111:107629.
[32] Abbasian AR, Shafiee Afarani M. One-step solution combustion synthesis and characterization of $ZnFe_2O_4$ and $ZnFe_{1.6}O_4$ nanoparticles. Applied Physics A. 2019;125(10):721.
[33] Rai M, Ingle AP, Gupta IR, Birla SS, Yadav AP, Abd-Elsalam KA. Potential role of biological systems in formation of nanoparticles: mechanism of synthesis and biomedical applications. Curr Nanosci. 2013;9(6):576-87.
[34] Lercher JA, Gründling C, Eder-Mirth G. Infrared studies of the surface acidity of oxides and zeolites using adsorbed probe molecules. Catalysis Today. 1996;27(3):353-76.
[35] Sternik D, Majdan M, Deryło-Marczewska A, Żukociński G, Gładysz-Płaska A, Gun'ko VM, et al. Influence of Basic Red 1 dye adsorption on thermal stability of Na-clinoptilolite and Na-bentonite. Journal of Thermal Analysis and Calorimetry J Therm Anal Calorim. 2011;103(2):607-15.
[36] Cheng Y, Wang L-J, Li J-S, Yang Y-C, Sun X-Y. Preparation and characterization of nanosized ZSM-5 zeolites in the absence of organic template. Materials Letters. 2005;59(27):3427-30.
[37] Jaleh B, Khalilipour A, Habibi S, Niyaifar M, Nasrollahzadeh M. Synthesis, characterization, magnetic and catalytic properties of graphene oxide/Fe_3O_4. Journal of Materials Science: Materials in Electronics. 2017;28(6):4974-83.
[38] Jadhav SA, Khedkar MV, Somvanshi SB, Jadhav KM. Magnetically retrievable nanoscale nickel ferrites: An active photocatalyst for toxic dye removal applications. Ceramics International. 2021;47(20):28623-33.
[39] Sun L, Zhang R, Wang Z, Ju L, Cao E, Zhang Y. Structural, dielectric and magnetic properties of $NiFe_2O_4$ prepared via sol–gel auto-combustion method. Journal of Magnetism and Magnetic Materials. 2017;421:65-70.
[40] Kombaiah K, Vijaya JJ, Kennedy LJ, Kaviyarasu K. Catalytic studies of $NiFe_2O_4$ nanoparticles prepared by conventional and microwave combustion method. Materials Chemistry and Physics. 2019;221:11-28.
[41] Ahangaran F, Hassanzadeh A, Nouri S. Surface modification of Fe_3O_4@SiO_2 microsphere by silane coupling agent. International Nano Letters. 2013;3(1):23.
[42] Zhang Y-F, Qiu L-G, Yuan Y-P, Zhu Y-J, Jiang X, Xiao J-D. Magnetic Fe_3O_4@C/Cu and Fe_3O_4@CuO core–shell composites constructed from MOF-based materials and their photocatalytic properties under visible light. Applied Catalysis B: Environmental. 2014;144:863-9.
[43] Saikia P, Miah AT, Das PP. Highly efficient catalytic reductive degradation of various organic dyes by Au/CeO_2-TiO_2nano-hybrid. Journal of Chemical Sciences. 2017;129(1):81-93.
[44] Ghosh BK, Hazra S, Naik B, Ghosh NN. Preparation of Cu nanoparticle loaded SBA-15 and their excellent catalytic activity in reduction of variety of dyes. Powder Technology. 2015;269:371-8.
[45] Yang X, Zhong H, Zhu Y, Jiang H, Shen J, Huang J, et al. Highly efficient reusable catalyst based on silicon nanowire arrays decorated with copper nanoparticles. Journal of Materials Chemistry A. 2014;2(24):9040-7.
[46] Gan Z, Zhao A, Zhang M, Tao W, Guo H, Gao Q, et al. Controlled synthesis of Au-loaded Fe_3O_4@C composite microspheres with superior SERS detection and catalytic degradation abilities for organic dyes. Dalton Transactions. 2013;42(24):8597-605.